JOURNAL OF BACTERIOLOGY, Apr. 1994, p. 2033–2043
0021-9193/94/$04.00+0

Vol. 176, No. 7

Rhizobium meliloti Contains a Novel Second Homolog of the Cell Division Gene *ftsZ*

WILLIAM MARGOLIN*† AND SHARON R. LONG

Department of Biological Sciences, Stanford University, Stanford, California 94305-5020

Received 11 October 1993/Accepted 28 January 1994

We have identified a second homolog of the cell division gene, *ftsZ*, in the endosymbiont *Rhizobium meliloti*. The *ftsZ2* gene was cloned by screening a genomic λ library with a probe derived from PCR amplification of a highly conserved domain. It encodes a 36-kDa protein which shares a high level of sequence similarity with the FtsZ proteins of *Escherichia coli* and *Bacillus subtilis* and FtsZ1 (Z1) of *R. meliloti* but lacks the carboxy-terminal region conserved in other FtsZ proteins. The identity of the *ftsZ2* gene product was confirmed both by in vitro transcription-translation in an *R. meliloti* S-30 extract and by overproduction in *R. meliloti* cells. As with Z1, the overproduction of FtsZ2 in *E. coli* inhibited cell division and induced filamentation, although to a lesser extent than with Z1. However, the expression of *ftsZ2* in *E. coli* under certain conditions caused some cells to coil dramatically, a phenotype not observed during Z1 overproduction. Although several Tn*3*-GUS (glucuronidase) insertions in a plasmid-borne *ftsZ2* gene failed to cross into the chromosome, one interruption in the chromosomal *ftsZ2* gene was isolated, suggesting that *ftsZ2* is nonessential for viability. The two *ftsZ* genes were genetically mapped to the *R. meliloti* main chromosome, approximately 100 kb apart.

The earliest known step in *Escherichia coli* cell division is the formation of a ring consisting of the FtsZ protein at the division site (5). FtsZ is also necessary for the formation of both vegetative and asymmetric sporulation septa in *Bacillus subtilis* (2). Cells containing very high levels of FtsZ or a temperature-sensitive FtsZ under nonpermissive conditions will form long, nonseptate filaments, presumably because the division ring cannot be formed (3, 39). It is not known how FtsZ, which is uniformly distributed during most of the cell cycle, assembles at the correct time in the center of the predivisional cell. However, the recent demonstrations that *E. coli* FtsZ binds GTP and has GTPase activity (10, 26, 29) suggest that GTP binding and hydrolysis by FtsZ could catalyze the assembly of the ring structure, in a manner analogous to filament formation by tubulins (34). The three previously sequenced FtsZ proteins, from *E. coli*, *B. subtilis*, and *Rhizobium meliloti* (1, 21, 40), all share a completely conserved 13-amino-acid domain that is very similar to the proposed GTP binding domain of tubulins (10), suggesting that GTP binding is a general feature of bacterial FtsZ proteins.

R. meliloti bacteria actively divide in free-living cultures and during infection of alfalfa roots, but they cease division and DNA replication and begin differentiating into bacteroids shortly after release into the plant cytoplasm (20). As part of our studies of the *R. meliloti* free-living and endosymbiotic phases, we previously characterized an *R. meliloti ftsZ* homolog that encoded a 63-kDa protein. Although this protein is very similar to the *E. coli* and *B. subtilis* FtsZ proteins, it also contains a 200-amino-acid insertion near the carboxy terminus which is rich in glutamine and proline (21). The presence of a very different FtsZ in *R. meliloti* implied that there may be considerable interspecific diversity of FtsZ structure and hence function. Here we characterize a novel, second *ftsZ* gene in *R. meliloti* that lacks both the 200-amino-acid insertion and a region at the carboxy terminus that is conserved in the three other FtsZ proteins characterized to date. We also show that this second *ftsZ* gene interferes with *E. coli* cell division when expressed, maps nearly 100 kilobase pairs (kb) away from the other *R. meliloti ftsZ* gene, and may be nonessential for *R. meliloti* viability.

* Corresponding author.

† Present address: Department of Microbiology and Molecular Genetics, University of Texas Medical School at Houston, Houston, TX 77030.

MATERIALS AND METHODS

Bacterial strains and plasmids. All strains and plasmids used in this study are listed in Table 1.

Bacterial growth and induction conditions. All *E. coli* strains were grown in Luria broth (LB) (30) plus 10 μg of tetracycline and 50 μg of ampicillin per ml for plasmids in host strain XL1-Blue. Isopropyl-β-D-thiogalactopyranoside (IPTG) inductions of *E. coli* cells were done by streaking colonies on agar plates containing LB, antibiotics, and 1 mM IPTG. *R. meliloti* cells were induced for protein overproduction by the addition of 1 mM IPTG to cells growing in LB plus 10 μg of tetracycline per ml in late exponential phase.

Preparation and manipulation of DNA. Restriction nucleases and T4 DNA ligase were from New England Biolabs. Klenow polymerase was from Amersham. DNA fragments were generally purified from agarose gels by the freeze-squeeze technique (37). Plasmid minipreparations obtained by alkaline or boiling extraction, large-scale plasmid preparations for S-30 reactions, and phage λ preparations were as described elsewhere (30). Total genomic DNA from *R. meliloti* was prepared as described previously (25).

Hybridizations. Southern hybridizations were performed essentially by the method of Church and Gilbert (7) at 65°C. Approximately 3 μg of total DNA from *R. meliloti* or *Agrobacterium tumefaciens* derivatives was isolated as described previously (25), digested overnight with a 10-fold excess of restriction enzyme, separated by agarose gel electrophoresis, and vacuum blotted to Magnagraph nylon membranes (Micron Separations Inc.). DNA was fixed to the membranes by baking at 80°C for 2 h and then hybridized. Radioactive DNA probes were made by random hexamer labeling with [α-^{32}P]dATP (Amersham) as described previously (14).

Isolation of an *ftsZ2* probe. An *ftsZ2*-specific template for

TABLE 1. Bacterial strains and plasmids used in this study

Strain of plasmid	Genotype or characteristics	Source or reference
Strains		
R. meliloti		
RCR2011	Wild type	25
Rm1021	Str^r derivative of RCR2011	25
R8501	Lac$^-$ derivative of Rm1021	G. Walker
Rm5000	SU47 Rif^r	J. Glazebrook
Rm6727	Tn*5*-Mob 601 linked to *leu-53*	19
Rm6743	Tn*5*-Mob 615 linked to *pyr-49*	19
Rm6761	Tn*5*-Mob 611 linked to *trp-33*	19
Rm5003	Rm5000 containing *met1023*::Tn*5*	J. Glazebrook
Rm7095	Rm1021 containing *exoR95*::Tn*5*	13
JAS171	Gm^r marker integrated into the Rm1021 chromosome	J. Swanson
WM249	Rm1021 Tn*5* mutant allowing efficient electroporation	41
WM320	pWM193 integrated into the R8501 chromosome	This work
WM321	pWM194 integrated into the R8501 chromosome	This work
WM329	pWM205 integrated into the R8501 chromosome	This work
WM331	pWM206 integrated into the R8501 chromosome	This work
WM358	Rm6727 transduced with Sp^r of WM329	This work
WM359	Rm6727 transduced with Sp^r of WM331	This work
E. coli		
XL1-Blue	*recA1 endA1 gyrA96 thi hsdR17 supE44 relA1 lac* (F′ *proAB lacI*^{q}ZΔM15 Tn*10*)	30; Stratagene
DH5α	*recA1 endA1 hsdR17 supE44 thi-1 gyrA relA1* Δ(*lacZYA-argF*)*U169 deoR* [ϕ80d*lac*Δ(*lacZ*)*M15*]	30
MT616	MM294A/pRK600 Cm^r	15
Plasmids		
pUC118	pUC18 containing the M13 replication origin	38
pUC119	pUC19 containing the M13 replication origin	38
pBluescript SK+	Ap^r vector containing the M13 replication origin	Stratagene
pZC9	Km^r version of pBR322	31
pM37	Source of Sp^r cassette	J. Mulligan
pSW213	Broad-host-range cloning vector with a multiple cloning site in *lacZ*	6
pJC05	Source of *ftsZ1* DNA	21
pWM132	*ftsZ2* PCR product cloned into *Eco*RV-cleaved pBluescript	This work
pWM139	3.5-kb *Sac*I fragment containing the 5′ end of *ftsZ2* cloned into pUC119	This work
pWM140	280-bp *Eco*RI-*Bam*HI fragment from pWM139 containing *ftsZ2* sequences cloned into *Eco*RI-*Bam*HI-cleaved pUC118	This work
pWM141	Like pWM140, but with the fragment cloned into pUC119	This work
pWM142	1.5-kb *Eco*RI fragment containing *ftsZ2* in pBluescript, in the orientation opposite that of the vector *lac* promoter	This work
pWM143	Like pWM142, but with *ftsZ2* in the opposite orientation	This work
pWM149	1.1-kb *Eco*RI-*Bam*HI fragment from pWM143 cloned into *Eco*RI-*Bam*HI-cleaved pUC118	This work
pWM164	1.4-kb *Sty*I-*Eco*RV fragment from pWM142 cloned into *Eco*RV-cleaved pBluescript	This work
pWM169	1.4-kb *Eco*RI-*Hin*dIII fragment from pWM164 cloned into pUC119 such that the *lac* promoter drives *ftsZ2* expression	This work
pWM176	pSW213 containing the *tac* promoter cloned into the *Cla*I site, oriented towards *lacZ*	This work
pWM186	pWM176 containing the *Cla*I-*Xba*I fragment from pWM169, such that the *tac* promoter drives *ftsZ2* expression	This work
pWM189	pWM176 containing the *Bam*HI-*Hin*dIII fragment from pJC06, such that the *tac* promoter drives *ftsZ1* expression	This work
pWM193	1.3-kb *Eco*RI-*Hin*dIII fragment from pWM149 cloned into *Eco*RI-*Hin*dIII-cleaved pZC9	This work
pWM194	0.3-kb *Bam*HI-*Sac*I fragment from pWM142 cloned into pZC9 cleaved with *Cla*I and filled in	This work
pWM204	0.4-kb *Eco*RI-*Hin*dIII fragment from pJC05 cloned into pZC9	This work
pWM205	*Hin*dIII-*Sal*I (Sp^r) fragment from pM37 replacing the 1.5-kb *Hin*dIII-*Sal*I (Nm^r) fragment from pWM194	This work
pWM206	*Hin*dIII-*Sal*I (Sp^r) fragment from pM37 replacing the 1.5-kb *Hin*dIII-*Sal*I (Nm^r) fragment from pWM204	This work

PCR amplification was isolated by size selecting gel-purified *Eco*RI fragments of about 1.5 kb from genomic DNA that weakly hybridized to an *ftsZ1* probe on a Southern blot (see Fig. 1). A conserved portion of *ftsZ2* was then specifically amplified from this size-selected DNA with the following PCR primers (kindly supplied by Y. V. Brun): 5′CTTGAATTCG C(G,C)AA(C,T)AC(G,C)GA(C,T)GC(G,C)CA(A,G)GC3′ to prime synthesis of the nontemplate strand and 3′TAC CC(G,C)CC(G,C)CC(G,C)TG(C,G)CC(C,G)TG(C,G)CC CCTAAGTTC5′ to prime synthesis of the template strand. These primers differ from the primers used to amplify *ftsZ1* (21) in that they are biased towards G+C, since the *R. meliloti* genome is 65% G+C. Although these primers contained terminal *Eco*RI sites, we obtained higher cloning efficiencies by filling in the ends and performing blunt-end ligations as described below.

PCRs were performed by use of a Hybaid thermal reactor (E&K Scientific) with a 20-μl reaction mixture containing 1× reaction buffer and 1 ml of Replinase enzyme (both supplied by NEN/DuPont), 500 pmol of each primer, 0.2 mM each deoxynucleoside triphosphate, and approximately 0.1 μg of template DNA. Each of 30 cycles of amplification consisted of denaturation at 95°C for 1 min, annealing at 50°C for 1 min, and polymerization at 74°C for 30 s. The PCR product was agarose gel purified, the ends were filled in with Klenow polymerase and deoxynucleoside triphosphates, and the product was cloned into *Eco*RV-cleaved pBluescript SK+ to make pWM132.

Screening of *R. meliloti* genomic libraries. The insert DNA in pWM132 was used to probe a λ library of *Bam*HI-digested *R. meliloti* genomic DNA as described previously (21). Positive plaques were purified, and bacteriophage DNA was isolated, digested with several restriction enzymes, and transferred to a Southern blot. The pWM132 probe hybridized to a 3.5-kb *Sac*I fragment, which was cloned for further analysis (pWM139). This clone was found to contain a 0.3-kb *Eco*RI-*Bam*HI fragment that hybridized to the probe, and examination of the DNA sequence of this fragment (in pWM140 and pWM141) indicated that only the 5′ portion of *ftsZ2* was present in the clone.

To obtain the full-length *ftsZ2* clone, we constructed a library of the same size-selected 1.5-kb *Eco*RI fragments of Rm1021 genomic DNA in pBluescript SK+. Blotting of bacterial colonies was done with nitrocellulose filters (Schleicher & Schuell, Inc.) as described previously (30). Two positively hybridizing clones were purified; they contained plasmids with a 1.5-kb *Eco*RI fragment in pBluescript in both orientations. These plasmids, pWM142 and pWM143, were used to make a series of subclones, which were subjected to DNA sequence analysis.

DNA sequencing and sequence analysis. The plasmids used for DNA sequencing were pWM142, pWM143, or subclones in pUC118, pUC119, or pBluescript; the host strain in all cases was XL1-Blue. Sequencing reactions were performed with the Sequenase version 2.0 kit (U.S. Biochemicals, Cleveland, Ohio) and [α-^{35}S]dATP. Single-stranded DNA was made by use of helper phage M13K07 as described elsewhere (16). DNA sequences were mapped and analyzed with University of Wisconsin Genetics Computer Group programs (10a); codon usage was examined with CODONPREFERENCE by use of a codon preference table compiled from 35 *R. meliloti* genes. Protein sequence alignment was performed with the PILEUP program.

Construction of *ftsZ* expression plasmids. To improve *ftsZ2* expression, we constructed plasmid pWM169 by deleting an 85-bp *Eco*RI-*Sty*I fragment from pWM142 immediately upstream from the ribosome binding site of *ftsZ2* (pWM164), then fusing the vector *lac* promoter directly to the *ftsZ2* translational start sequences by recloning into pUC119. To strongly induce gene expression in *R. meliloti*, we modified the broad-host-range plasmid pSW213, which carries the *lac* promoter and the *lac* repressor (6); the inducible *tac* promoter, which is a much stronger promoter in *E. coli* than is the *lac* promoter, was cloned into the *Cla*I site of the pSW213 polylinker, in the same orientation as the *lac* promoter (pWM176). The *ftsZ1* and *ftsZ2* genes were cloned into pWM176 by use of the 2-kb *Bam*HI-*Hin*dIII fragment of pJC06 (21) and the 1.4-kb *Cla*I-*Xba*I fragment of pWM169 to make pWM189 and pWM186, respectively. Derivatives of *R. meliloti* Rm1021 (WM249) and *E. coli* XL1-Blue were used for *ftsZ* expression studies; WM249, unlike Rm1021, contains a mutation allowing it to efficiently accept *E. coli* DNA by electroporation (41).

In vitro protein synthesis. Coupled transcription-translation reactions with S-30 extracts from *R. meliloti* RCR2011 and 1 μg of the appropriate CsCl-banded plasmid DNA template were performed as described previously (16). Labeled proteins were analyzed as described previously (21).

Construction of *ftsZ*-linked drug resistance markers. Our strategy was to link each *ftsZ* gene with an Nm^r or an Sp^r marker on an *R. meliloti* suicide plasmid and then to force single-crossover recombination to create a tandem duplication and mark chromosomal *ftsZ*. The 0.4-kb *Hin*dIII-*Eco*RI fragment of pJC05, carrying a region downstream of *ftsZ1* (21), and the 0.3-kb *Bam*HI-*Sac*I fragment of pWM142, carrying an internal segment of *ftsZ2* near the N terminus, were cloned into Nm^r plasmid pZC9 (31), which can be mated into but cannot be maintained in *R. meliloti*. Plasmid pZC9 is pBR322 with its *Hin*dIII-*Sal*I fragment within the Tc^r gene replaced by the *Hin*dIII-*Sal*I fragment encoding Nm^r from Tn*5*. The resulting plasmids, pWM194 and pWM204, carried Nm^r linked to *ftsZ2* and *ftsZ1*, respectively. The Nm^r cassette in pWM194 and pWM204 was swapped for Sp^r by replacement with the 2.2-kb *Hin*dIII-*Sal*I fragment from pRmM37 (27), creating pWM205 and pWM206, respectively. Both pWM194 and pWM205 carry a small internal segment of *ftsZ2*, designed such that single-crossover recombination should lead to an interruption of chromosomal *ftsZ2*, with vector sequences inserted between the *Bam*HI and *Sac*I sites.

To transfer all four of these plasmids into Rm8501, a derivative of Rm1021 (24), we performed triparental matings with MT616 (12). After growth on LB agar at 30°C overnight, the mating mixtures were plated on LB agar containing streptomycin plus spectinomycin or LB agar containing streptomycin plus neomycin to select for Sp^r or Nm^r recombinants, respectively.

Genetic mapping. To map *ftsZ1* with respect to *ftsZ2*, the transducing phage N3 (24) was grown on the appropriate Nm^r or Sp^r strain and used to transduce recipient strains marked with the other drug resistance; transductants were then screened for loss of the recipient marker.

To map the *ftsZ* genes roughly with respect to other chromosomal markers, we used conjugational mapping with several *oriT*::Tn*5* insertions in the *R. meliloti* chromosome (19). First, Sp^r markers linked to *ftsZ1* and *ftsZ2* were transduced into the *oriT*::Tn*5* strains Rm6727, Rm6743, and 6761. These Sp^r Nm^r strains were then triparentally conjugated into JAS171, an Rm1021 derivative marked with Gm^r, and the relative frequency of Gm^r Sp^r exconjugants was determined. Donors for finer-level conjugational mapping were derivatives of Rm6727, WM358 and WM359, containing Sp^r-linked *ftsZ2* and *ftsZ1*, respectively. Recipients were JAS171 derivatives into which Tn*5* markers from Rm7095 and Rm5003 had been transduced. Exconjugants were selected on LB agar plates containing streptomycin, gentamicin, and spectinomycin and then patched on LB agar containing streptomycin, gentamicin, and spectinomycin and LB agar containing streptomycin, gentamicin, spectinomycin, and neomycin; the percentage of recipients which became Nm^s was scored. For fine-structure mapping, Rm5003 was transduced with Sp^r-linked *ftsZ1* and *ftsZ2*, and transductants were scored for Nm^s.

RESULTS

Isolation of a second *R. meliloti ftsZ* gene. An additional *ftsZ* locus, *ftsZ2*, was originally suggested by weakly hybridizing secondary bands in an *R. meliloti* genomic Southern blot

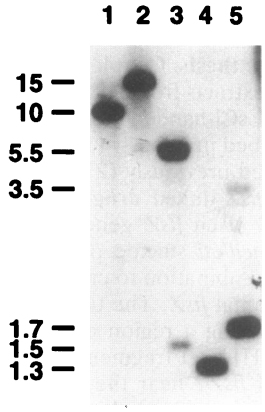

FIG. 1. Detection of a second *ftsZ* gene in *R. meliloti*. A Southern blot was made with restriction digests of total DNA from Rm1021 as described in Materials and Methods, probed with the portion of *ftsZ1* DNA amplified by PCR (21), and autoradiographed. DNAs were digested with *Bam*HI (lane 1), *Bgl*II (lane 2), *Eco*RI (lane 3), *Pst*I (lane 4), and *Sac*I (lane 5). The sizes of selected bands in comparison with size markers are indicated to the left in kilobases.

probed with a portion of the *ftsZ1* gene (Fig. 1). We did not detect specific bands corresponding to more than two copies, suggesting that no more than two copies of *ftsZ* are present. To isolate and characterize this potential *ftsZ* homolog, we size selected DNA corresponding to one of the secondary hybridization signals and obtained a 1.5-kb *Eco*RI fragment. A highly conserved region of the new homolog, *ftsZ2*, was then PCR amplified, as was done previously for *ftsZ1* (21). We isolated a partial *ftsZ2* clone by screening a λ library of *Bam*HI-digested *R. meliloti* DNA with the *ftsZ2*-specific PCR product, also similar to our strategy for cloning *ftsZ1*. We were not able to find the remainder of the gene in the λ library, perhaps because of the large size of the downstream *Bam*HI fragment, which would have prevented its packaging. Therefore, we constructed a size-selected plasmid library of *R. meliloti* DNA and screened it with the cloned PCR product to obtain the full-length gene. The restriction map of a 1.5-kb *Eco*RI fragment containing the entire *ftsZ2* gene is shown in Fig. 2. The nucleotide sequence of the *Eco*RI fragment, shown in Fig. 3, encodes a single open reading frame for a 345-amino-acid protein preceded by a strong ribosome binding site.

Despite overall similarities, there are major structural differences between FtsZ1 (Z1) and FtsZ2 (Z2) and between the two *R. meliloti* FtsZ proteins and their *E. coli* and *B. subtilis* homologs. The predicted Z2 protein, at 36 kDa, is significantly smaller than the 40-kDa *E. coli* and *B. subtilis* homologs. As shown in the four-way alignment in Fig. 4, the difference in size in large part reflects the absence of the carboxy-terminal domain shared by the other three proteins. Z2 is highly similar to the others in the amino-terminal half, including a 13-amino-acid perfect match around the putative GTP binding sequence shared by the other three proteins (10). This identity strongly

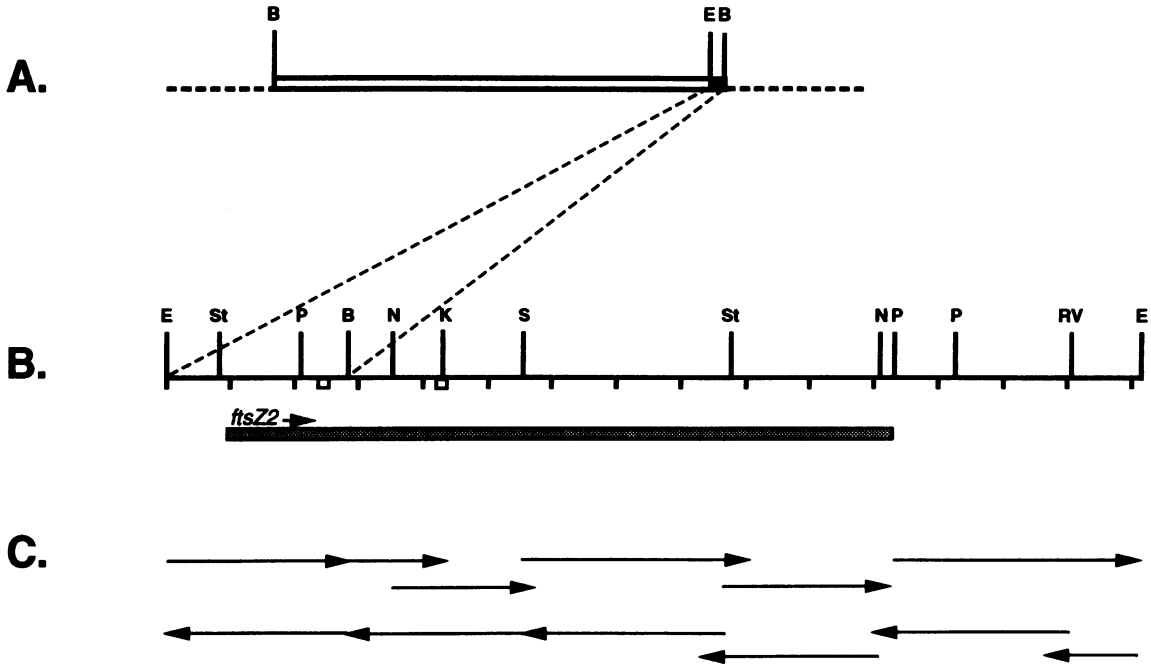

FIG. 2. Physical characterization of *ftsZ2*. (A) Depiction of the λ clone containing the portion of *ftsZ2* that hybridized to the PCR product. The box represents a large *Bam*HI insert cloned into λ GEM-11. The broken lines on either side represent the λ arms. The filled E-B segment contains the beginning of the *ftsZ2* open reading frame and is expanded in panel B. Vertical lines represent the locations of restriction enzyme cleavage sites (B, *Bam*HI; E, *Eco*RI). (B) Restriction map of the *ftsZ2* region. The heavy line represents the 1.5-kb *Eco*RI fragment isolated from the plasmid library (pWM142 and pWM143). Vertical tick marks below the heavy line show 100-bp intervals. Vertical lines above the heavy line denote restriction enzyme cleavage sites (B, *Bam*HI; E, *Eco*RI; K, *Kpn*I; N, *Not*I; P, *Pst*I; RV, *Eco*RV; S, *Sac*I; St, *Sty*I). The two open boxes below the heavy line represent the positions of the PCR primers used to initially amplify this sequence. The hatched bar and arrow depict the predicted *ftsZ2* open reading frame and direction. (C) Sequencing strategy. Arrows denote the direction and extent of the DNA sequence obtained with various subclones of pWM142 and pWM143.

```
      EcoRI
   1  GAATTCCTAGAATGAAAGCGCCTGATTCGCGCCGCACCGCATACGATCTCCGTGTTCCGA
  61  GTTTTCGGGCGGCCGGGGAACTGCCCAAGGAGAAGAACCATGACGGAATACAAGAAGCCG
                                                  M  T  E  Y  K  K  P
 121  ATCATTACCGAGATGCGCCCGAAGATCACGGTCATCGGCGTCGGCGGCGGCGGCGGCAAC
      I  I  T  E  M  R  P  K  I  T  V  I  G  V  G  G  G  G  G  N

 181  GCGATCAACAACATGATCGCCGAAAACCTGCAGGGCGTCGATTTCATCGCCGCAAACACG
      A  I  N  N  M  I  A  E  N  L  Q  G  V  D  F  I  A  A  N  T

 241  GACGCGCAGGCGCTGGCGACATCGAAGGCGGAGCGGCGGATCCAACTGGGCGCTGCCATC
      D  A  Q  A  L  A  T  S  K  A  E  R  R  I  Q  L  G  A  A  I

 301  ACCGAGGGTCTCGGCGCCGGTTCGGTGCCCGACATCGGCAATGCGGCCGCCCAGGAATCG
      T  E  G  L  G  A  G  S  V  P  D  I  G  N  A  A  A  Q  E  S

 361  ATCGACGAGATCATGGATCACCTCGGCGGCACGCATATGTGCTTCGTCACGGCAGGCATG
      I  D  E  I  M  D  H  L  G  G  T  H  M  C  F  V  T  A  G  M

 421  GGCGGCGGTACCGGTACGGGAGCGGCGCCGGTGATCGCGGAAGCGGCGCGGCGGGCCGGC
      G  G  G  T  G  T  G  A  A  P  V  I  A  E  A  A  R  R  A  G

 481  ATCCTGACGGTTGCGGTCGTCACCAAGCCCTTCAGCTTCGAGGGACAGCGGCGCATGCAG
      I  L  T  V  A  V  V  T  K  P  F  S  F  E  G  Q  R  R  M  Q

 541  ACGGCGGAGCTCGGCGTCGAGCGGCTGCGGGAGAGCGCAGACACGGTCATCGTCATCCCC
      T  A  E  L  G  V  E  R  L  R  E  S  A  D  T  V  I  V  I  P

 601  AACCAGAACCTCTTTCGCATCGCCGATGCCAAGACGACCTTCGCCGACGCATTCATGATT
      N  Q  N  L  F  R  I  A  D  A  K  T  T  F  A  D  A  F  M  I

 661  GCCGACCGGGTCCTCTATTCGGGGGTCAGCTGCATCACCGACCTGATCGTCAAGGAGGGG
      A  D  R  V  L  Y  S  G  V  S  C  I  T  D  L  I  V  K  E  G

 721  CTGATGAATCTCGACTTCGCCGACGTCAAGACGGTGATGAAGGGCATGGGCCGGGCGATG
      L  M  N  L  D  F  A  D  V  K  T  V  M  K  G  M  G  R  A  M

 781  ATGGGCACGGGCGAAGCGACCGGCGAGAACCGGGCGATGCTGGCGGCGGAAGCGGCGATC
      M  G  T  G  E  A  T  G  E  N  R  A  M  L  A  A  E  A  A  I

 841  GCCAACCCGCTGCTCGACGAAGTCTCCATGCGCGGTGCCAAGGGCGTCCTCGTGTCGATC
      A  N  P  L  L  D  E  V  S  M  R  G  A  K  G  V  L  V  S  I

 901  TCCGGCGGCATGGACATGACGCTTTTCGAGGTGGACGAGGCGGCGACCCGCATCCGCGAG
      S  G  G  M  D  M  T  L  F  E  V  D  E  A  A  T  R  I  R  E

 961  GAAGTTTACGACGAGGCCGACATCGTCGTCGGCGCGATCTTCGACCGGAGCCTGGACGGC
      E  V  Y  D  E  A  D  I  V  V  G  A  I  F  D  R  S  L  D  G

1021  ACTTTCCGCGTGTCCGTCGCGACCGGCCTCGACAGCAACCGCAGCGCCCAGCCGACGGCG
      T  F  R  V  S  V  A  T  G  L  D  S  N  R  S  A  Q  P  T  A

1081  CCGGAGGCCATGAACGGCCAGACGGCGGCCGCCGTTCCTTCGCGTACGCTGCAGTAGGAT
      P  E  A  M  N  G  Q  T  A  A  A  V  P  S  R  T  L  Q  *

1141  AGCGGATACGGCGGATGCCCCCGTACGGGGGAGATGTCACGAAAGTGACAAACGGGTGCG
1201  AGTTTTCAGGAAACACAACACTACTGCAGTTTGCCCCTCTCCTCGGGTTAAACCCGAGGA
1261  CTAGCCCTCTCCCCGCAAGCGGGGAGGGGGGACGTGCCTGATCGGGCACATCCCATTCCA
1321  AGCAATCTGGCGGAGGCAACAGAGCGCTGCGAGTCCCTTCGCCCCGCTTGCGGGGAGAAG
1381  GTGCCGGCAGGCGGATGAGGGGCGGGTCTTTCGGCAGCAGCTGGATATCAGTCAGGCAGG
1441  CCGGCGCGGTGCAGATCGCGGACGAAACGATCGATGAAATCTTCCGGCATGACCGGCACG
1501  CTGCCGAAGTAGAATTC  1517
            EcoRI
```

FIG. 3. DNA sequence and predicted protein sequence of the *R. meliloti ftsZ2* gene. The nucleotide sequence of the 1.5-kb *Eco*RI fragment of pWM143 containing the entire *ftsZ2* gene is shown. The deduced sequence of the Z2 protein is shown in single-letter amino acid code below the nucleotide sequence, with the asterisk denoting the amber stop codon. The predicted ribosome binding site for *ftsZ2* is underlined.

suggests that both *R. meliloti* FtsZ proteins are GTPases. The conservation at the amino terminus and the divergence toward the carboxy terminus are also clear for Z1, which has near the carboxy terminus 200 extra residues that are strikingly hydrophilic and enriched for proline and glutamine. It is notable that 12 of the last 27 carboxy-terminal residues of Z2 are identical to a portion of the Z1 insertion region (Fig. 4). This similarity between Z1 and Z2 is underscored by the fact that despite their large size differences, Z1 and Z2 are approximately 70% identical. By comparison, Z2 is 47% identical to *E. coli* FtsZ and 49% identical to *B. subtilis* FtsZ. The *E. coli* and *B. subtilis* FtsZ proteins are 52% identical to each other. Z1 displays 50

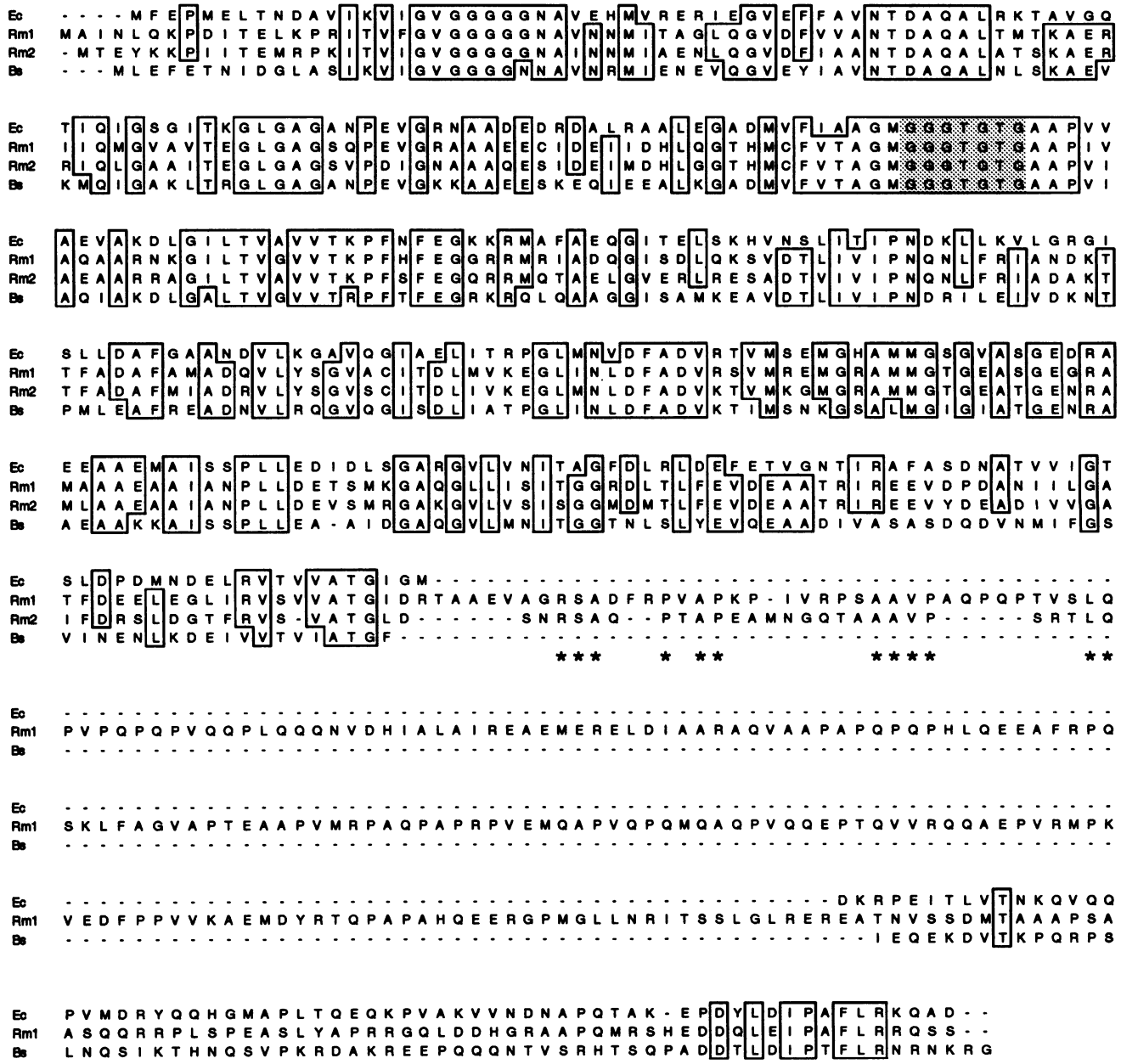

FIG. 4. Alignment of the four characterized bacterial FtsZ proteins. Single-letter amino acid codes are shown. Ec, *E. coli* (40); Rm1, *R. meliloti* Z1 (21); Rm2, *R. meliloti* Z2; Bs, *B. subtilis* (1). Residues at the same position are boxed if both *R. meliloti* proteins and at least one other protein share identity. Asterisks below the alignment denote amino acid identities between the C terminus of Z2 and an internal segment of Z1. The shaded region represents homology to the tubulin signature motif suggested to be a GTP binding domain (10). The alignment was first done with the PILEUP program and then optimized manually. The single-letter amino acid codes are as follows: A, Ala; C, Cys; D, Asp; E, Glu; F, Phe; G, Gly; H, His; I, Ile; K, Lys; L, Leu; M, Met; N, Asn; P, Pro; Q, Gln; R, Arg; S, Ser; T, Thr; V, Val; W, Trp; and Y, Tyr.

and 53% identities to *E. coli* FtsZ and *B. subtilis* FtsZ, respectively.

The composition of the Z2 protein is also similar to that of the other FtsZ proteins, with several exceptions. Z2 shares the large proportion (over 22 mol%) of alanine and glycine residues found in the other three FtsZ proteins, as well as the lack of any tryptophan residues (21). Its estimated pI of 4.6 is similar to the very low pIs (all under 5) for the others (21). However, while the *E. coli* and *B. subtilis* FtsZ proteins lack cysteines, both *R. meliloti* FtsZ proteins contain cysteines at residues 101 and 198 (Z2 coordinates); Z1 contains at position 87 (Z2 coordinates) an additional cysteine which corresponds to a serine in Z2. Future biochemical analyses of structure and function should shed light on these structural features.

Identification of the Z2 protein product. We were interested in confirming the identity of the *ftsZ2* gene product and determining whether *ftsZ2* might be expressed in *R. meliloti*. The *ftsZ1* gene is expressed in *R. meliloti* cells, since Z1 can be detected with an antibody directed against *E. coli* FtsZ (23). However, this antibody failed to detect Z2 unless it was present

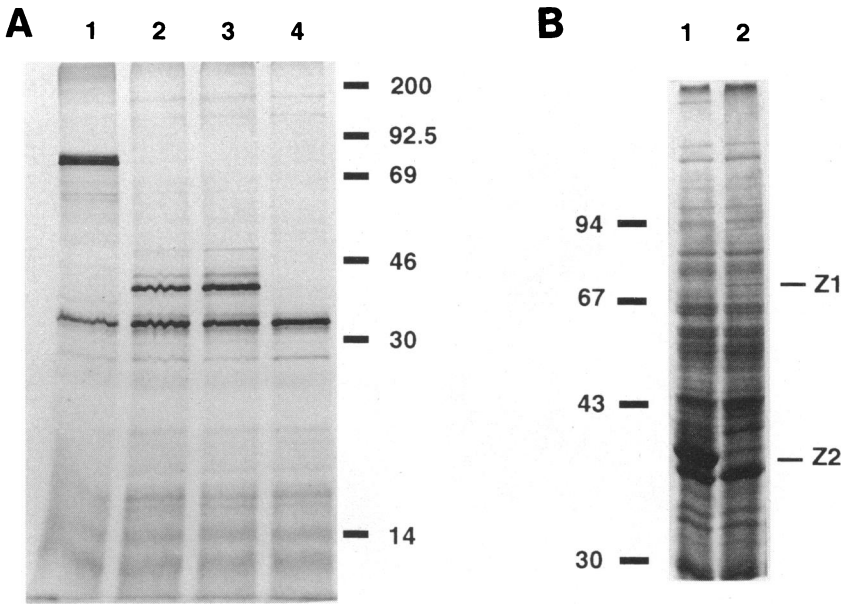

FIG. 5. Plasmid-directed synthesis of FtsZ proteins in *R. meliloti*. (A) Synthesis of [^{35}S]methionine-labeled protein in *R. meliloti* S-30 extracts. Protein was made from the following pBluescript SK+-derived DNA templates: pJC06 (21), expressing *ftsZ1* (lane 1); pWM142, with *ftsZ2* in an orientation opposite that of the *lac* promoter (lane 2); pWM143, with *ftsZ2* in the same orientation as the *lac* promoter (lane 3); and pBluescript SK+ alone (lane 4). A portion of each reaction mixture was subjected to SDS-polyacrylamide gel electrophoresis and autoradiographed as described previously (21). The positions of ^{14}C-labeled protein standards are indicated on the right (in kilodaltons). The 32-kDa band in all the lanes is the vector-encoded β-lactamase. (B) Overproduction of Z2 (lane 1) and Z1 (lane 2) in *R. meliloti*. Cells containing pWM186 (lane 1) or pWM189 (lane 2) were induced with 1 mM IPTG as described in Materials and Methods, concentrated, sonicated, resuspended in sample buffer (2% SDS, 5% β-mercaptoethanol, 10% glycerol, 0.1% bromophenol blue), separated on an SDS–10% polyacrylamide gel, and stained with Coomassie brilliant blue. Protein markers (in kilodaltons) are shown on the left, and arrows point to the overproduced FtsZ bands.

at very high levels after overproduction from plasmid pWM186 in *R. meliloti*, and even then the level of detection was poor (data not shown). This result suggested that the majority of the epitopes recognized by the antibody were near the carboxy terminus, rendering it a poor probe for immunoblotting. In addition, a truncated derivative of Z1 expressed from pJ062, which harbored a deletion of the carboxy-terminal domain also missing in Z2 (21), was not detectable on immunoblots (data not shown). These findings are consistent with the lack of immunoreactivity that we observed for Z2 on Western blots (immunoblots).

Two indirect lines of evidence suggest that *ftsZ2* is expressed in vivo. First, *ftsZ2* codon usage was analyzed. Using an *R. meliloti* codon usage data base containing 35 genes and setting the rare-codon threshold at 0.10, we identified 85 rare codons reading from left to right in the 1.5-kb *Eco*RI fragment containing *ftsZ2*, yet none were found in the *ftsZ2* open reading frame. Similarly, *ftsZ1* contained no rare codons. Both genes are also preceded by strong ribosome binding site sequences. The other evidence for *ftsZ2* expression in vivo comes from our in vitro studies of *ftsZ2* expression. We used an *R. meliloti*-derived coupled transcription-translation system to synthesize the Z2 protein from two *ftsZ2*-containing plasmids (pWM142 and pWM143). The predicted 36-kDa Z2 protein was synthesized in vitro as efficiently as the Z1 protein (Fig. 5A), suggesting that Z2 is similarly synthesized efficiently in vivo. Unlike Z1, which migrates as several close bands on sodium dodecyl sulfate (SDS) gels and which migrates more slowly than predicted (21), Z2 migrates as a single band at its predicted molecular mass. In addition, the efficient synthesis of Z2 in either orientation with respect to the vector suggests that an *R. meliloti* promoter lies immediately upstream of *ftsZ2*.

We confirmed the identity of the *ftsZ2* gene product by overproducing a 36-kDa protein to high levels in *R. meliloti* cells after induction of the strong *tac* promoter on pWM186, which contains the cloned *ftsZ2* gene (Fig. 5B). Z1 was also overproduced in an analogous construct (pWM189), but at much lower levels. The 36-kDa band was purified, and an amino-terminal protein sequence analysis confirmed that it corresponded to Z2 (data not shown).

It therefore seems likely, on the basis of these criteria, that *ftsZ2* directs the synthesis of a 36-kDa protein during some phase of *R. meliloti* growth. However, definite proof that Z2 is synthesized in *R. meliloti* cells must await isolation of the homologous antiserum.

Effects of *ftsZ2* expression on *E. coli*. To determine whether Z2 affects cell division, we assayed the effects of *R. meliloti* *ftsZ2* expression on *E. coli*. The overproduction of *E. coli* FtsZ or *R. meliloti* Z1 in *E. coli* inhibits division, causing cell filamentation (21, 39). The mechanism of this inhibition is unknown but may involve an alteration of the proper ratio between FtsZ and the essential cell division protein FtsA, since increased levels of FtsA can suppress the *E. coli* FtsZ overproduction phenotype (9, 11). In contrast, a lower level of expression of *R. meliloti* Z1 or *E. coli* FtsZ in *E. coli* causes the production of smaller cells, which probably arise because of increased division frequency (21).

We overproduced Z2 in *E. coli* by inducing a *lac* promoter-*ftsZ2* plasmid with IPTG. IPTG-induced levels of Z2 induced filamentation (Fig. 6B), suggesting that FtsZ ring assembly was abnormal. The lower level of expression obtained in the absence of IPTG yielded two surprising results. First, we observed moderate filamentation instead of division stimulation. Second, this lower level of expression also caused a

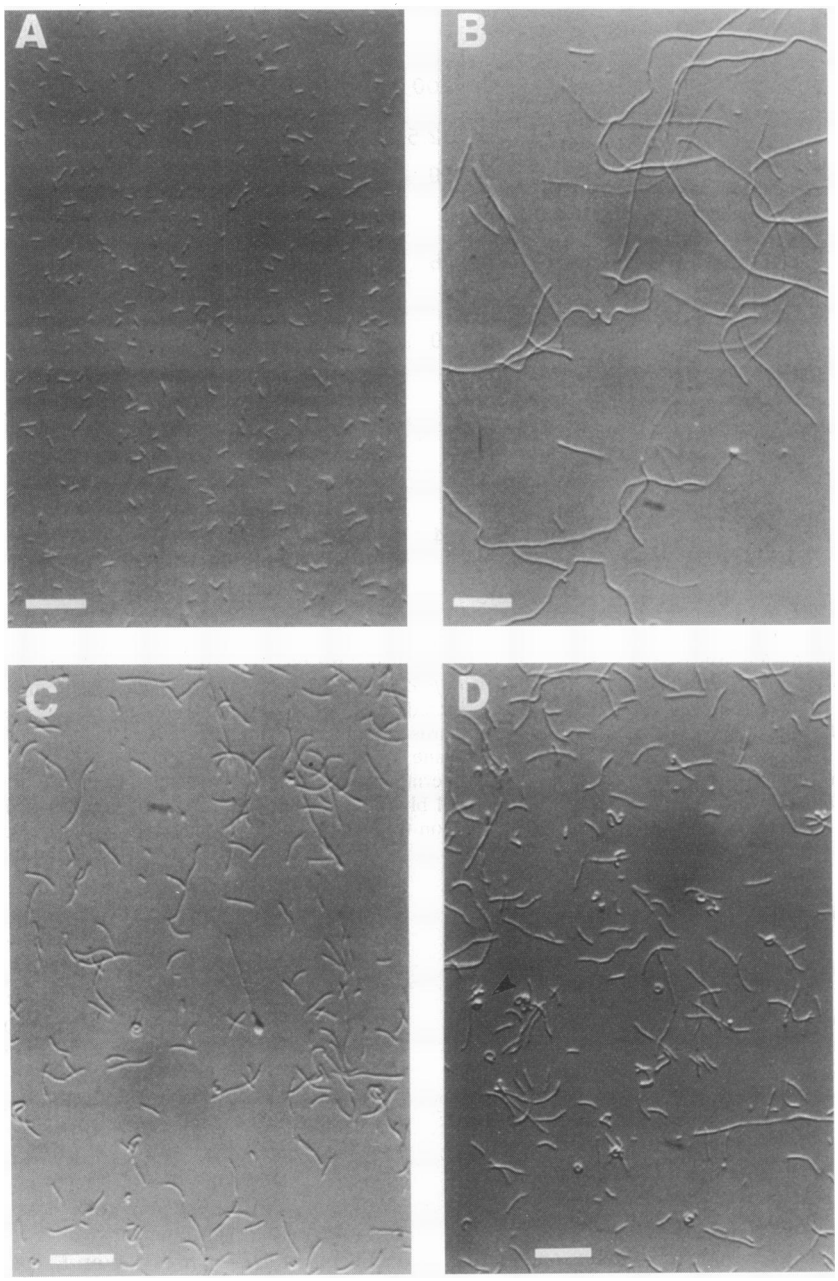

FIG. 6. Effects of expression of *ftsZ2* on *E. coli* cells. Derivatives of *E. coli* XL1-Blue (*lacI*^{q}) carrying pBluescript (A) or pBluescript derivatives with the vector *lac* promoter driving the transcription of *ftsZ2* (pWM169) (B to D) were grown at 37°C on LB plates with 1 mM IPTG (A and B) or no IPTG (C and D). Plasmid pWM169 is a derivative of pWM143 in which the 85-bp *Eco*RI-*Sty*I fragment upstream of the *ftsZ2* coding region is deleted, resulting in a higher level of expression (see Materials and Methods). Cells were viewed with a Nikon light microscope with Nomarski optics. Photographs were taken with a Nikon FE-35 camera and Kodak Ektachrome film (160 ASA). Bars, 20 μm.

portion of the cells to become comma shaped (Fig. 6C and D). These cells appeared to have extended one side at the expense of the other, resulting in tightly coiled rods instead of straight rods. This differential extension must occur across the entire length of a cell in a regular manner to result in such uniform coils. Similar morphologies were recently observed during the expression of a mutant *E. coli ftsA* gene (17), suggesting that this phenotype could be caused by an altered interaction between FtsA and FtsZ. The coiling and kinking were also seen within longer filaments (Fig. 6B), in contrast to the straight filaments obtained from the overproduction of Z1 (21). In addition, a small number of these filamentous cells containing Z2 bulged at one pole (Fig. 6D, arrowhead). These results suggest that the overproduction of Z2 inhibits cell division but also causes asymmetric growth patterns not observed with Z1 overproduction. Therefore, Z1 and Z2 appear to have different effects on *E. coli* morphology when overproduced. Neither *ftsZ1* nor *ftsZ2* was able to complement a temperature-sensitive *E. coli ftsZ* mutant, JFL101 (data not shown).

Construction of *ftsZ* insertions. We were interested in knowing whether one or both *ftsZ* genes are essential for *R.*

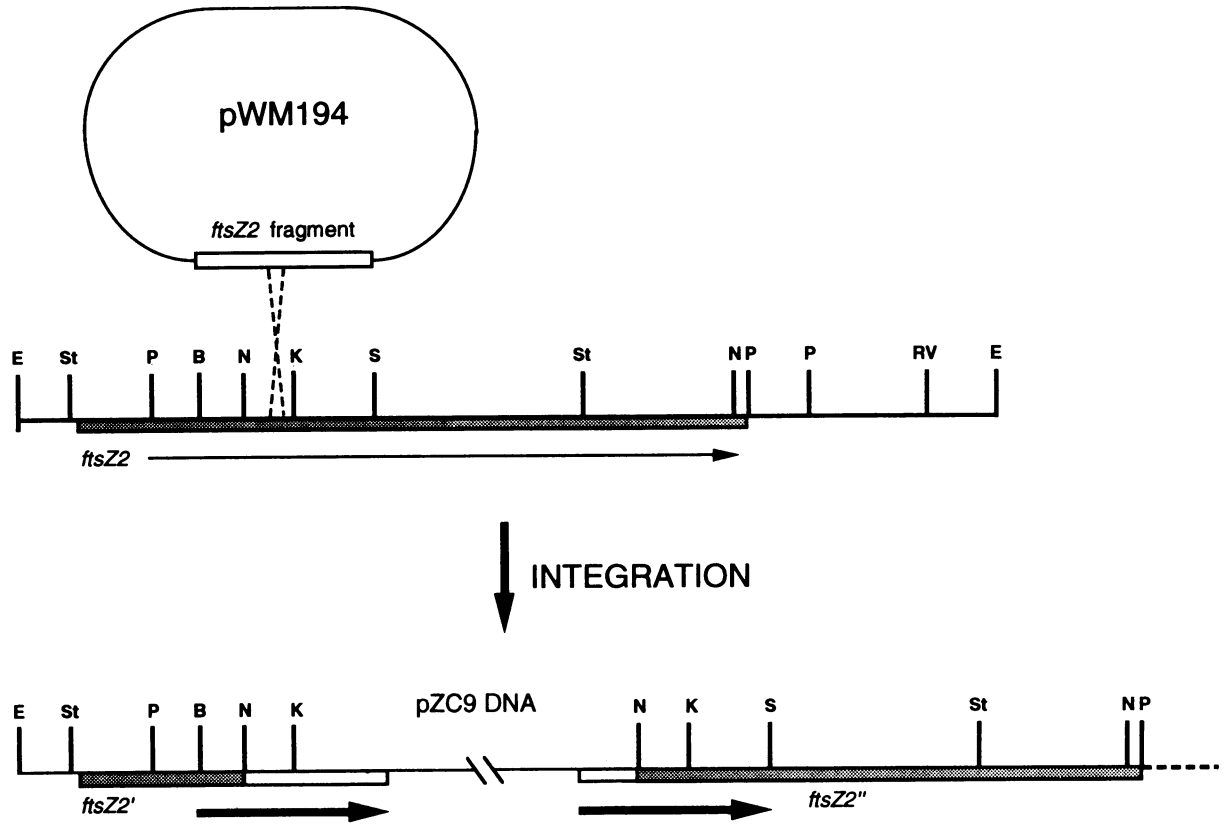

FIG. 7. Schematic representation of single-crossover recombination to yield an insertion in *ftsZ2*. At the top is shown pZC9 derivative pWM194, containing the original *Bam*HI-*Sac*I fragment internal to *ftsZ2* (open box). The proposed single crossover with *R. meliloti* chromosomal *ftsZ2* is denoted by broken lines. As in Fig. 2, the *ftsZ2* open reading frame is shown as a hatched bar, with the orientation of *ftsZ2* transcription represented by an arrow underneath. Restriction sites and symbols are as explained in the legend to Fig. 2. At the bottom is shown the structure resulting from the recombination event. Interrupted portions of *ftsZ2* are denoted as *ftsZ2'* and *ftsZ2"*. Heavy arrows below the line indicate the portions of DNA that have been tandemly duplicated.

meliloti growth, as are the *E. coli* and *B. subtilis ftsZ* genes (2, 8). We constructed insertions containing drug resistance markers on plasmid-borne copies of both *ftsZ1* and *ftsZ2* and then attempted to recombine these with the chromosomal copies to determine whether either chromosomal copy of *ftsZ* could be interrupted and still result in a viable cell. Our first approach was to randomly insert the Tn*3*-HoHoGUS element (36) into plasmids containing *ftsZ2* and *ftsZ1*, mate these constructs into Rm1021, and then attempt to cross the insertion into the chromosome. Although several insertions were isolated in both genes, none could be introduced into the chromosomal copies by double crossover (data not shown). In an alternate approach, we took advantage of the ability of pBR322 derivatives to be conjugated into but not to replicate in Rm1021 by making insertions in *ftsZ* via Campbell recombination (single crossover). Donor molecules that contained a DNA fragment either internal to *ftsZ* or adjacent to *ftsZ* were constructed. Upon Campbell recombination into the bacterial chromosome, the internal fragment would result in the insertion of the vector containing an Nm^r marker flanked by a tandem duplication, while the external fragment would result in the Nm^r marker being linked closely to the gene and also flanked by a tandem duplication (Fig. 7). The donor plasmids were then mated into Rm1021, and Nm^r exconjugants were isolated for all constructs except that containing the interruption in *ftsZ1*. Sp^r cassettes were introduced within *ftsZ2* and adjacent to *ftsZ1* by the same method. The presence of an Nm^r or an Sp^r cassette within *ftsZ2* was confirmed by Southern blot analysis (data not shown), and the viability of the cells containing the insertion suggests that *ftsZ2* is nonessential for growth in free-living cultures. Likewise, our ability to isolate a linked marker but not an insertion for *ftsZ1* suggests that *ftsZ1* is essential for free-living growth.

Location of the two *ftsZ* genes on the *R. meliloti* main chromosome. *R. meliloti* is unusual in that it has three major replicons: a main chromosome and two large symbiotic megaplasmids (35). In addition, there are several examples of multigene families in *R. meliloti*. They may be linked, such as the three *nodD* copies located within 25 kb on one megaplasmid (18), or divided among multiple replicons, such as the two *nodPQ* loci involved in the synthesis of Nod factors (32, 33) and the two *groESL* chaperonin loci (28). With the precedent of multigene families varying in location, we were interested in determining the location of the two *ftsZ* genes. A preliminary physical analysis indicated that both genes were chromosomally encoded (data not shown). Using the *ftsZ1*-linked marker and *ftsZ2* insertion marker described above, we mapped both *ftsZ* genes by generalized phage transduction (see Materials and Methods) to within approximately 100 kb on the main chromosome (Table 2). This is the first case of duplicated genes both mapping to the main chromosome of *R. meliloti*. In addition, we used conjugational mapping to map the *ftsZ* genes

TABLE 2. Genetic linkage analysis of *ftsZ* genes of *R. meliloti*

Donor strain[a]	Recipient strain[a]	% of Nm^r transductants that were Sp^s	% of Sp^r transductants that were Nm^s	Linkage (kb)[b]
WM321 (*ftsZ2*-Nm^r)	WM329 (*ftsZ2*-Sp^r)	100		0
WM321 (*ftsZ2*-Nm^r)	WM331 (*ftsZ1*-Sp^r)	5		100
WM329 (*ftsZ2*-Sp^r)	WM321 (*ftsZ2*-Nm^r)		100	0
WM331 (*ftsZ1*-Sp^r)	WM321 (*ftsZ2*-Nm^r)		10	85
WM329 (*ftsZ2*-Sp^r)	*met-1023*::Tn*5* (Nm^r)		0	>140
WM331 (*ftsZ1*-Sp^r)	*met-1023*::Tn*5* (Nm^r)		36	46

[a] *R. meliloti* strains are described in Table 1. Phage N3 was grown on donor strains and then used to transduce recipient strains to Sp^r or Nm^r.

[b] Calculated from the Wu equation (39a): linkage = $160 - 160(\%/100)^{0.333}$, where % = the percentage of marker replacement. The approximate size of the N3 genome is 160 kb.

roughly to other chromosomal markers (see Materials and Methods) and determined by transduction that *ftsZ1* maps near the *met-1023* locus (Table 2).

We also were interested in knowing whether both *ftsZ* genes were in sequence contexts similar to those of *E. coli* and *B. subtilis*, in which *ftsZ* is downstream of the cell division gene *ftsA* in an operon (1, 40). We identified an *R. meliloti* homolog of *ftsA* just upstream of *ftsZ1*; however, we could not detect a second locus of *ftsA* by hybridization, and sequencing upstream of *ftsZ2* did not reveal any similarity to *ftsA* (22). Therefore, *ftsZ2* appears to be in a completely unique sequence context.

DISCUSSION

FtsZ is a structural protein that has GTPase activity and that is essential for the initiation of bacterial cell division. *E. coli* and *B. subtilis* each have single-copy *ftsZ* genes which have been well characterized and are highly similar in size and structure (1, 40). In this paper, a continuation of our study of *R. meliloti* cell division, we have described the first characterization of a bacterial *ftsZ* two-gene family. Although the *R. meliloti* FtsZ proteins share similar domains with the other FtsZ proteins, their divergence from the *E. coli* and *B. subtilis* FtsZ proteins and from each other near the carboxy terminus suggests that bacterial FtsZ proteins may be quite structurally diverse. There is good evidence, obtained with mutant FtsZ proteins, that the GGGTGTG domain near the amino terminus is required for GTP binding and function (10, 26, 29). However, it is likely that other FtsZ domains have important roles in ring formation and disassembly and in interactions with other cell division components that have yet to be elucidated. An analysis of common protein sequence domains should be a valuable tool in addition to a mutant analysis for understanding more about FtsZ structure and function, particularly in diverse bacteria.

The presence of more than one *ftsZ* gene in *R. meliloti* is unprecedented and suggests that the regulation or structural contribution of FtsZ in *R. meliloti* cell division may differ from that in *E. coli* and *B. subtilis*. For example, the very different upstream DNA sequences of *ftsZ1* and *ftsZ2* hint at the possibility of differential transcriptional regulation. The different structural properties of Z1 and Z2 suggest that when either is synthesized alone, division rings should have different properties; likewise, when they are present together, they may form mixed multimers, similar to the mixed multimers proposed to explain the effects of the *ftsZ3* allele in *E. coli* (4).

We were not able to complement an *E. coli ftsZ84* mutant with either *ftsZ1* or *ftsZ2*. This result could have been due to an improper level of Z1 or Z2, the failure of Z1 or Z2 to form division rings in the heterologous host, or perhaps a dominant negative effect by the mutant *E. coli* protein that would prevent ring formation by *R. meliloti* FtsZ. It is possible that the inhibition of *E. coli* cell division under certain conditions by high levels of Z2 is a nonspecific stress response. However, the coiled cell phenotype observed with *ftsZ2* expression is unusual and implies a specific effect of Z2 on *E. coli* cell wall growth. Altered forms of FtsA also cause *E. coli* to adopt a coil morphology (17), and thin sections of these cells show what appear to be multiple septa extending diagonally across the cells instead of one perpendicular septum. The similar *E. coli* morphologies due to perturbations of FtsA or FtsZ are intriguing in light of the possible interaction between the two proteins. The FtsZ-FtsA interaction is supported by the observation that the filamentous phenotype obtained during FtsZ overproduction in *E. coli* can be suppressed by a corresponding overproduction of FtsA (9, 11). This observation suggests that the coil morphology of *E. coli* expressing *ftsZ2* may be caused by an unusual interaction between Z2 and FtsA. The Z2 protein, as a naturally occurring altered form of FtsZ, should prove useful in probing further details of *E. coli* cell division and morphology, the relationship of FtsZ structure to function, and the potential interaction between FtsA and FtsZ.

Although its DNA sequence features and efficient expression in an S-30 system suggest that *ftsZ2* is expressed in *R. meliloti*, we could not immunologically detect the Z2 protein in *R. meliloti* cultures. There are several possible explanations for this result. First, the antibody recognizes Z2 poorly after SDS-polyacrylamide gel electrophoresis, since only an overproduced protein that is clearly visible as a Coomassie brilliant blue-stained band can be detected; thus even if Z2 levels were as high as those of *E. coli* FtsZ (about 20,000 monomers per rapidly growing cell) (5), Z2 might not be detectable in whole-cell extracts. Second, *ftsZ2* may be expressed only under certain conditions, for example, in the differentiated bacteroid state within the nodule. This possibility necessitates an analysis of expression in plant tissues. The location of *ftsZ2* so far from *ftsZ1*, *ftsA*, and perhaps other cell division genes suggests that if this gene is expressed at all, its expression may be uncoupled from that of other cell division genes. Third, *ftsZ2* may be inactive, despite its excellent codon usage. This inactivity is consistent with our ability to obtain viable cells containing an interruption of chromosomal *ftsZ2* but not *ftsZ1*. This result suggests that while *ftsZ1* may be essential for free-living growth, *ftsZ2* may not be. It is likely that at least one *ftsZ* gene in *R. meliloti* is essential, since the *ftsZ* genes of *E. coli* and *B. subtilis* have been shown to be essential for viability, on the basis of the construction of conditional null mutations (2, 8). However, *ftsZ2* could still be an essential gene, since several other attempts at interrupting chromosomal *ftsZ2* were unsuccessful, and we cannot rule out the possibility that our WM205 strain containing the *ftsZ2* interruption acquired a linked suppressor (an unlinked one is unlikely, since the interruption

could be transduced to a new strain). Future studies of the expression and function of both *R. meliloti* FtsZ proteins, as well as FtsZ proteins in other bacteria, should allow a better understanding of the role of FtsZ in initiating cell division.

ACKNOWLEDGMENTS

We thank members of the Long laboratory for helpful discussions, D. Ehrhardt for help with microscopic techniques, D. Bramhill for the λ library, J. Corbo for genomic DNAs, R. Fisher, T. Egelhoff, J. Ogawa, and M. Yelton for the S-30 extracts, and G. Kalinowski, J. A. Downie, and R. Fisher for useful comments on the manuscript.

This research was supported by USDA grant 88-37262-3978. W.M. was additionally supported by a National Science Foundation Postdoctoral Fellowship in Plant Biology.

REFERENCES

1. **Beall, B., M. Lowe, and J. Lutkenhaus.** 1988. Cloning and characterization of *Bacillus subtilis* homologs of *Escherichia coli* cell division genes *ftsZ* and *ftsA*. J. Bacteriol. **170:**4855–4864.
2. **Beall, B., and J. Lutkenhaus.** 1991. FtsZ in *Bacillus subtilis* is required for vegetative septation and for asymmetric septation during sporulation. Genes Dev. **5:**447–455.
3. **Begg, K. J., and W. D. Donachie.** 1985. Cell shape and division in *Escherichia coli*: experiments with shape and division mutants. J. Bacteriol. **163:**615–622.
4. **Bi, E., and J. Lutkenhaus.** 1990. Analysis of *ftsZ* mutations that confer resistance to the cell division inhibitor SulA (SfiA). J. Bacteriol. **172:**5602–5609.
5. **Bi, E., and J. Lutkenhaus.** 1991. FtsZ ring structure associated with division in *Escherichia coli*. Nature (London) **354:**161–164.
6. **Chen, C.-Y., and S. C. Winans.** 1991. Controlled expression of the transcriptional activator gene *virG* in *Agrobacterium tumefaciens* by using the *Escherichia coli lac* promoter. J. Bacteriol. **173:**1139–1144.
7. **Church, G. M., and W. Gilbert.** 1984. Genomic sequencing. Proc. Natl. Acad. Sci. USA **81:**1991–1995.
8. **Dai, K., and J. Lutkenhaus.** 1991. *ftsZ* is an essential cell division gene in *Escherichia coli*. J. Bacteriol. **173:**3500–3506.
9. **Dai, K., and J. Lutkenhaus.** 1992. The proper ratio of FtsZ to FtsA is required for cell division to occur in *Escherichia coli*. J. Bacteriol. **174:**6145–6151.
10. **de Boer, P., R. Crossley, and L. Rothfield.** 1992. The essential bacterial cell-division protein FtsZ is a GTPase. Nature (London) **359:**254–256.

10a. **Devereaux, J., P. Haeberli, and O. Smithies.** 1984. A comprehensive set of sequence analysis programs for the VAX. Nucleic Acids Res. **12:**387–395.

11. **Dewar, S. J., K. J. Begg, and W. D. Donachie.** 1992. Inhibition of cell division initiation by an imbalance in the ratio of FtsA to FtsZ. J. Bacteriol. **174:**6314–6316.
12. **Ditta, G., S. Stanfield, D. Corbin, and D. R. Helinski.** 1980. Broad host range DNA cloning system for gram-negative bacteria: construction of a gene bank of *Rhizobium meliloti*. Proc. Natl. Acad. Sci. USA **77:**7347–7351.
13. **Doherty, D., J. A. Leigh, J. Glazebrook, and G. C. Walker.** 1988. *Rhizobium meliloti* mutants that overproduce the *R. meliloti* acidic Calcofluor-binding exopolysaccharide. J. Bacteriol. **170:**4249–4256.
14. **Feinberg, A. P., and B. Vogelstein.** 1983. A technique for radiolabeling DNA restriction endonuclease fragments to high specific activity. Anal. Biochem. **132:**6–13.
15. **Finan, T. M., B. Kunkel, G. F. De Vos, and E. R. Signer.** 1986. Second symbiotic megaplasmid in *Rhizobium meliloti* carrying exopolysaccharide and thiamine synthesis genes. J. Bacteriol. **167:**66–72.
16. **Fisher, R. F., J. A. Swanson, J. T. Mulligan, and S. R. Long.** 1987. Extended region of nodulation genes in *Rhizobium meliloti* 1021. II. Nucleotide sequence, transcription start sites and protein products. Genetics **117:**191–201.
17. **Gayda, R. C., M. C. Henk, and D. Leong.** 1992. C-shaped cells caused by expression of an *ftsA* mutation in *Escherichia coli*. J. Bacteriol. **174:**5362–5370.
18. **Honma, M. A., M. Asomaning, and F. M. Ausubel.** 1990. *Rhizobium meliloti nodD* genes mediate host-specific activation of *nodABC*. J. Bacteriol. **172:**901–911.
19. **Klein, S., K. Lohman, R. Clover, G. C. Walker, and E. R. Signer.** 1992. A directional, high-frequency chromosomal mobilization system for genetic mapping of *Rhizobium meliloti*. J. Bacteriol. **174:**324–326.
20. **Long, S. R.** 1989. *Rhizobium*-legume nodulation: life together in the underground. Cell **56:**203–214.
21. **Margolin, W., J. C. Corbo, and S. R. Long.** 1991. Cloning and characterization of a *Rhizobium meliloti* homolog of the *Escherichia coli* cell division gene *ftsZ*. J. Bacteriol. **173:**5822–5830.
22. **Margolin, W., and S. R. Long.** Unpublished data.
23. **Margolin, W., and S. R. Long.** Unpublished data.
24. **Martin, M. O., and S. R. Long.** 1984. Generalized transduction in *Rhizobium meliloti*. J. Bacteriol. **159:**125–129.
25. **Meade, H. M., S. R. Long, G. B. Ruvkun, S. E. Brown, and F. M. Ausubel.** 1982. Physical and genetic characterization of symbiotic and auxotrophic mutants of *Rhizobium meliloti* induced by transposon Tn*5* mutagenesis. J. Bacteriol. **149:**114–122.
26. **Mukherjee, A., K. Dai, and J. Lutkenhaus.** 1993. *Escherichia coli* cell division protein FtsZ is a guanine nucleotide binding protein. Proc. Natl. Acad. Sci. USA **90:**1053–1057.
27. **Mulligan, J. T., and S. R. Long.** 1985. Induction of *Rhizobium meliloti nodC* expression by plant exudate requires *nodD*. Proc. Natl. Acad. Sci. USA **82:**6609–6613.
28. **Ogawa, J., and S. R. Long.** Unpublished data.
29. **Raychaudhuri, D., and J. T. Park.** 1992. *Escherichia coli* cell-division gene *ftsZ* encodes a novel GTP-binding protein. Nature (London) **359:**251–254.
30. **Sambrook, J., E. F. Fritsch, and T. Maniatis.** 1989. Molecular cloning: a laboratory manual, 2nd ed. Cold Spring Harbor Laboratory Press, Cold Spring Harbor, N.Y.
31. **Schwedock, J., and S. R. Long.** 1989. Nucleotide sequence and protein products of two new nodulation genes of *Rhizobium meliloti*, *nodP* and *nodQ*. Mol. Plant-Microbe Interact. **2:**181–194.
32. **Schwedock, J., and S. R. Long.** 1990. ATP sulphurylase activity of the *nodP* and *nodQ* gene products of *Rhizobium meliloti*. Nature (London) **348:**644–647.
33. **Schwedock, J. S.** 1991. Characterization of *Rhizobium meliloti nodP* and *nodQ*, nodulation genes that encode ATP sulfurylase. Ph.D. thesis. Stanford University, Stanford, Calif.
34. **Snyder, J. A., and J. R. McIntosh.** 1976. Annu. Rev. Biochem. **45:**699–720.
35. **Sobral, B. W. S., R. J. Honeycutt, A. G. Atherly, and M. McClelland.** 1991. Electrophoretic separation of the three *Rhizobium meliloti* replicons. J. Bacteriol. **173:**5173–5180.
36. **Swanson, J. A., J. T. Mulligan, and S. R. Long.** 1993. Regulation of *syrM* and *nodD3* in *Rhizobium meliloti*. Genetics **134:**435–444.
37. **Tautz, D., and M. Renz.** 1983. An optimized freeze-squeeze method for the recovery of DNA fragments from agarose gels. Anal. Biochem. **132:**14–19.
38. **Vieira, J., and J. Messing.** 1987. Production of single-stranded plasmid DNA. Methods Enzymol. **153:**3–11.
39. **Ward, J. E., and J. Lutkenhaus.** 1985. Overproduction of FtsZ induces minicells in *E. coli*. Cell **42:**941–949.

39a. **Wu, T. T.** 1966. A model for three-point analysis of random general transduction. Genetics **54:**405–410.

40. **Yi, Q.-M., S. Rockenbach, J. E. Ward, and J. Lutkenhaus.** 1985. Structure and expression of the cell division genes *ftsQ*, *ftsA*, and *ftsZ*. J. Mol. Biol. **184:**399–412.
41. **Zumstein, L., W. Margolin, and S. R. Long.** Unpublished data.